JPE 16-2-29

http://dx.doi.org/10.6113/JPE.2016.16.2.695
ISSN(Print): 1598-2092 / ISSN(Online): 2093-4718

Design of a Fuel Cell Power Conditioning System for Online Diagnosis and Load Leveling

Thanh-Tuan Nguyen*, Van-Tuan Doan*, and Woojin Choi†
*,†Department of Electrical Engineering, Soongsil University, Seoul, Korea

Abstract

A fuel cell power conditioning system for online diagnosis and load leveling under the condition of varying load is developed in this study. The proposed system comprises a unidirectional boost converter and a bidirectional buck–boost converter with a battery. The system operates in two different modes. In normal mode, the bidirectional converter is utilized for load leveling; in diagnostic mode, it is utilized to control load voltage while the boost converter generates perturbation current to implement the online diagnosis function through in-situ electrochemical impedance spectroscopy (EIS). The proposed method can perform EIS for a fuel cell under varying-load conditions with no influence on the load. The validity and feasibility of the proposed system are verified by experiments, and the design procedure of the proposed system is detailed.

Key words: EIS, Electrochemical impedance spectroscopy, Fuel cell, Load leveling, Online diagnosis

I. INTRODUCTION

Although fuel cells are emerging as a viable energy source, their proliferation is hindered by two main drawbacks, namely, limited overload-handling capability and unknown lifespan. A power-conditioning system for fuel cells needs to be designed to compensate for such drawbacks and make systems associated with fuel cells reliable power sources [1], [2]. Owing to its inherent characteristics, a fuel cell requires a start-up time and has a limited overload-handling capability. When a fuel processor is utilized for fuel cells, a long delay cannot be avoided. This delay prevents the fuel cell from providing instantaneous supply of sufficient power for the load at start-up. The response of a fuel cell system mainly depends on several factors, such as hydrogen and air supply, mass flow, temperature and pressure control, and heat and water management [3], [4]. According to previous research, the limited overload-handling capability and long start-up time of fuel cells can be overcome by using a hybrid topology with an energy storage device, such as a battery or supercapacitor [1, 2, 5, 6]. Compared with a fuel cell, a battery and a supercapacitor demonstrate a rapid response with no start-up time, and their power density is much higher than that of fuel cells. Therefore, if a battery is employed as an auxiliary energy storage device, the system can exhibit stable operation under fast dynamic load and instantaneous overload conditions.

The unknown lifespan of fuel cell power systems is another concern. This uncertainty may reduce the reliability of the system. A fuel cell degrades as the operation hours accumulate and eventually reaches its end of life (EOL). However, given that a fuel cell depends on many factors, such as operating condition and load pattern, the performance degradation of a fuel cell is more serious than expected; it may also fail suddenly. Hence, detecting the aging of fuel cells and prognosticating their EOL are important to prevent the sudden failure of fuel cell power systems. Many studies have evaluated the performance and estimated the lifespan of fuel cells to develop reliable methods to estimate their state of health (SOH) [7]-[12]. In [8], a model-based fault diagnosis method for a proton exchange membrane (PEM) fuel cell was developed with computing residuals as indicators. In this method, the analytical relationships between inputs and outputs are obtained by using a physical model of the system. This method can approximate any type of continuous nonlinear function without knowledge of the physical processes of the fuel cell system. However, high-quality data describing the entire process should be utilized to ensure the accuracy of the diagnosis result. Another useful technique for the diagnosis and prognosis of fuel cells is electrochemical impedance spectroscopy (EIS) because it helps characterize the electrochemical performance and investigate the fundamental

Manuscript received Jul. 31, 2015; accepted Jan. 26, 2016
Recommended for publication by Associate Editor Jonghoon Kim.
†Corresponding Author: cwj777@ssu.ac.kr
Tel: +82-2-820-0652, Fax: +82-2-817-7961, Soongsil University
*Department of Electrical Engineering, Soongsil University, Korea

process of fuel cells, that is, their SOH [9]-[11], [13]. Reference [9] proposed a method to accurately estimate the SOH of a fuel cell in operation using the time constant calculated from the extracted parameters of the equivalent circuit model of the fuel cell through EIS. Investigation of the variation in the equivalent circuit parameter values over the operation time of 2200 h has shown that the time constant for the cathode, a product of electric double-layer capacitance and charge transfer resistance that represents the reduction reaction of the cathode, is a reliable parameter to evaluate the degradation of a fuel cell. Thus, if the EIS function is integrated with a power conditioning system for a fuel cell, it can be a useful tool to monitor the SOH of the fuel cell by periodically monitoring the variation in the equivalent circuit parameter values, thereby making the fuel cell power system highly reliable. However, the EIS function cannot be integrated with a power conditioning system when conventional converter topologies and control methods are utilized because the EIS operation should be performed independently without disturbing the load, and load variation should not affect the EIS operation. Considering that the output voltage and current of the converter should be regulated with no influence from perturbation during EIS operation, an auxiliary energy storage device is required to compensate for the power difference between the fuel cell and the load [14]. In typical applications, given that the power demand by the load varies according to the load profile scenario, perturbation of the fuel cell for EIS and load variation should be completely decoupled from each other.

In this study, a power-conditioning system for fuel cell diagnosis and load leveling under varying-load conditions is developed. The proposed system comprises two converters, namely, a main converter to supply fuel cell power to the load and a bidirectional converter for diagnosis and load leveling. In normal mode operation, an additional bidirectional converter with an associated auxiliary battery is utilized for load leveling; in the diagnostic mode operation, it is utilized to implement the diagnosis function through EIS. The EIS function can be implemented by generating a frequency-swept small current perturbation from the fuel cell through the current controller of the main boost converter. The impedance spectrum of the fuel cell over the frequency range of interest is calculated by the digital lock-in amplifier (DLIA) embedded in a digital signal processor (DSP). The EIS data are then utilized to extract the parameters of the fuel cell equivalent circuit model; the variation is subsequently utilized to evaluate the SOH of the fuel cell.

II. Proposed Power-Conditioning System For Fuel Cell Diagnosis and Load Leveling

Fig. 1 shows a block diagram of the power-conditioning system with the diagnosis function for the fuel cell and the load

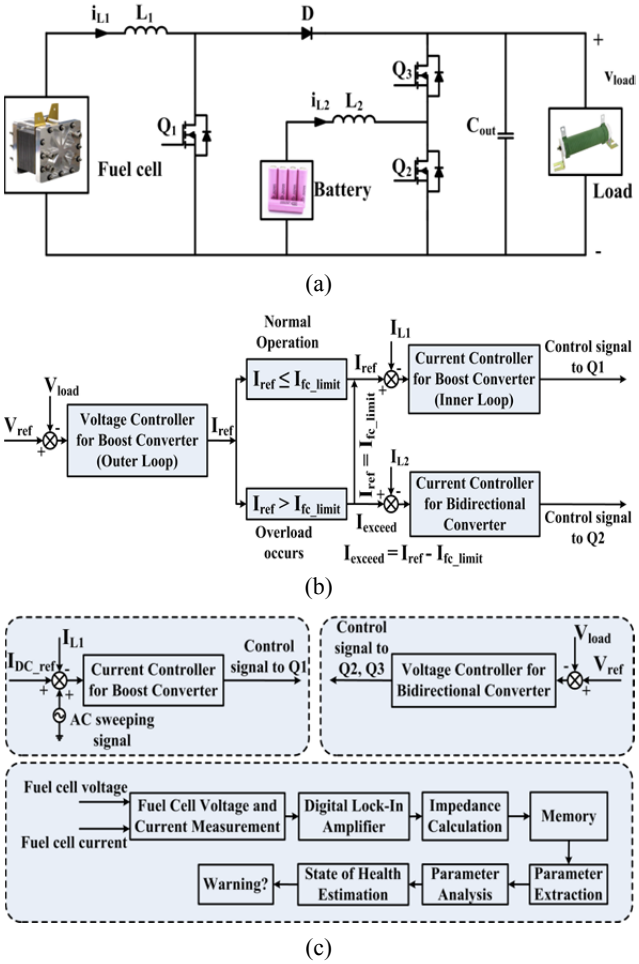

(a) (b) (c)

Fig. 1. Control scheme of the proposed power conditioning system for fuel cell diagnosis and load leveling. (a) Power conditioning system. (b) Normal operation with load leveling. (c) EIS operation for diagnosis.

leveling function under the condition of varying load. The power converter consists of a conventional boost converter associated with the fuel cell and a bidirectional converter associated with an auxiliary battery.

In normal mode operation, the boost converter regulates the load voltage at the desired value, and the bidirectional converter is used to handle abrupt load changes or instantaneous overload. Load leveling compensates for the load power with the power from the auxiliary energy storage device if the power from the fuel cell is insufficient for the full load. If the power from the fuel cell is larger than the required power for the load, the excess power is used to charge the battery. The diagnostic mode is regularly performed to investigate the SOH of the fuel cell. In this mode, the boost converter performs fuel cell current control to generate frequency-swept current perturbation for the EIS operation, and the bidirectional converter regulates the output voltage. During EIS mode, the operation of the boost converter has to be decoupled from that of the bidirectional converter to ensure the success of impedance measurements regardless of the load variation. Thus,

in this mode, the boost converter draws a small alternating current (AC) perturbation over the frequency range of interest superimposed on a certain direct current (DC) offset value, and the bidirectional converter regulates the load voltage by charging and discharging the battery associated with it. Within a perturbation cycle, the battery is charged when the perturbation current becomes higher than the DC offset and discharged when the current declines to below the DC offset to keep the output voltage constant.

When the fuel cell is perturbed by a small sinusoidal current, its voltage response with respect to the current perturbation is then measured over the frequency range of interest. The DLIA embedded in the DSP is utilized to calculate the in-phase and quadrature-phase components of the current perturbation and its voltage response. The AC impedance of the fuel cell at each frequency is also calculated. The equivalent circuit parameters of the fuel cell are extracted from the measured impedance data by using the complex nonlinear least square (CNLS) fitting technique. The extracted parameters are used to evaluate the degradation and/or the SOH of the fuel cell by comparing them to the initial parameter values of the fuel cell when it was fresh.

III. Diagnosis of the Fuel Cell under Varying-Load Conditions by Using Online EIS

A. Fuel Cell Degradation and its Lifespan Estimation Method

EIS is widely utilized to obtain AC impedance data of the fuel cell over the frequency range of interest, which can be represented by the Nyquist plot. The AC impedance data are then further processed with an equivalent circuit model of the fuel cell to extract the equivalent circuit parameters that can be used to evaluate the soundness of the fuel cell.

Various equivalent circuit models of the fuel cell can be used to analyze the AC impedance spectrum obtained through the EIS method depending on such factors as measurement object, operating point of the system, and frequency range of measurements [9, 15–19]. Typical equivalent circuit models of the fuel cell are composed of resistance, electric double-layer capacitance, and Warburg impedance. The resistance component includes the ion resistance of electrolytes, the electric resistance of components, and the charge transfer resistance [9]. In this study, a simple equivalent circuit model of the fuel cell composed of membrane resistance, charge transfer resistance, and electric double-layer capacitance is utilized to extract the parameters, as shown in Fig. 2.

The electrochemical process of the fuel cell can be divided into two major reactions, namely, hydrogen oxidation in the anode and oxygen reduction in the cathode. Each reaction is represented by a semicircle on the Nyquist impedance plane. However, given that the reaction rate of hydrogen oxidation is much faster than that of oxygen reduction, the semi-circle

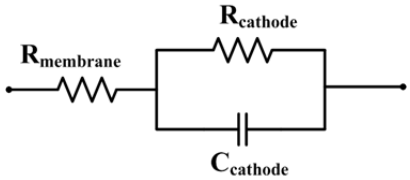

Fig. 2. Equivalent circuit model of the PEM fuel cell used for parameter extraction.

representing oxygen reduction is dominant in the Nyquist impedance plot. Thus, the equivalent circuit parameters for the cathode can be observed only by using the model in Fig. 2 to estimate the SOH of the fuel cell.

Previous research has indicated that the degradation of a fuel cell mainly occurs in the cathode catalyst because of catalyst dissolution, precipitation, aging, catalyst particle movement, and carbon support corrosion [20], [21]. Catalyst particles are condensed by dissolution and precipitation reactions to reduce the surface energy, thereby decreasing the area of the three-phase interface, which is required for the reduction reaction; this scenario results in the degradation of the fuel cell. The reduction reaction rate is reduced by the decrease in electrochemical surface area. Hence, the charge transfer resistance value increases. The electric double-layer capacitance value in the three-phase interface decreases.

Considering that fuel cell degradation does not only increase the charge transfer resistance but also decrease the electric double-layer capacitance, the time constant, a product of the two parameters, is more accurate when used to judge the soundness of the fuel cell than using the two parameters individually [9]. This estimation method requires calculating the standard cathode time constant ($\tau_{cathode\_standard}$) with the cumulative operation time of the fuel cell in the test and the lifespan equation obtained by pretests. This method also requires calculating the cathode time constant ($\tau_{cathode}$) of the fuel cell stack in the test by using EIS and a parameter extraction technique at the time of inspection [9]. The ratio of the cathode time constant at operation time t with respect to the standard cathode time constant, time constant ratio $P_{ca}(t)$, can then be calculated with Equ. (1) and utilized to evaluate the SOH of the fuel cell, that is, the remaining lifetime.

$$P_{ca}(t) = \frac{\tau_{cathode}(t)}{\tau_{cathode\_standard}} \quad (1)$$

If the time constant ratio is equal to unity, then the condition of the fuel cell during the test is determined as fair. Otherwise, the fuel cell is in a good or poor condition if the time constant ratio is less or greater than unity, respectively. The ratio also can be utilized to calculate the remaining life of the fuel cell in use. The complete details of the procedure to evaluate the SOH and remaining life of the fuel cell stack are found in [9]. The technique to extract the parameters of the equivalent circuit model in Fig. 2, which are then utilized to calculate time constant ratio $P_{ca}(t)$, is discussed in the following section.

B. Impedance Measurement and Parameter Extraction Techniques Used for Fuel Cell Diagnosis

1) DLIA Technique: Small current perturbation at the frequency of interest is applied to the fuel cell to perform EIS on it. The voltage response is measured. For the test, the voltage response caused by the current perturbation should be lower than the thermal voltage to guarantee the linearity of the test, as shown below [3].

$$V_T = \frac{RT}{F} = 26mV \text{ at } 25^oC\,, \tag{2}$$

where R = 8.314 (J/mol-K), T = Temp (K), and F = 96485 (C/mol).

The current perturbation and voltage response are then measured with the DLIA method, which is widely utilized to extract small signals even in the presence of high noise levels [22]. The small input AC signal superimposed on a DC component and noise n(k) detected by DLIA can be expressed in a discrete form at the k^{th} sampling step as follows:

$$X[k] = DC + A\sin\left(2\pi\frac{f}{f_s}k + \theta\right) + n(k);\ \mathrm{k} = 0,1,2,\ldots\,. \tag{3}$$

In DLIA, the sine and cosine reference signals at the same frequency of interest are numerically generated by DSP, as shown in Equ. (4). The advantage of the numerically generated reference signal is that it can be immunized from noise [23].

$$S[k] = \sin\left(2\pi\frac{f}{f_s}k\right),\ C[k] = \cos\left(2\pi\frac{f}{f_s}k\right),\ \mathrm{k} = 0,1,2,\ldots \tag{4}$$

The detected signal is then multiplied by the sine and cosine reference signals to obtain the in-phase and quadrature-phase signals as Equs. (5) and (6).

By filtering the AC component in Equs. (5) and (6) and by using the moving average filter, the magnitude and phase of the target signal can be calculated, as shown in Equs. (7) and (8).

$$I[k] = X[k]\times S[k] = \frac{A}{2}\cos(\theta) + AC \text{ components} \tag{5}$$

$$Q[k] = X[k]\times C[k] = \frac{A}{2}\sin(\theta) + AC \text{ components} \tag{6}$$

$$x = 2\times I[k] \approx A\cos(\theta);\ y = 2\times Q[k] \approx A\sin(\theta) \tag{7}$$

$$M = \sqrt{x^2 + y^2} = A\ ;\ Ph = \tan^{-1}\left(\frac{y}{x}\right) = \theta \tag{8}$$

The complex impedance of the fuel cell can be presented as

$$Z(\omega_0) = R(\omega_0) + jX(\omega_0)\,. \tag{9}$$

2) CNLS Method for Parameter Extraction of the Fuel Cell Equivalent Circuit Model: The parameters of the equivalent circuit of the fuel cell must be obtained to estimate the SOH of the fuel cell. The parameters can be extracted with a least-square fitting algorithm. In this work, the CNLS fitting method is utilized to estimate the values of the equivalent circuit parameters of the fuel cell. The CNLS fitting method is a type of the Levenberg–Marquardt least-square method, which can be applied to complex numbers. The method requires the measured impedance data of the fuel cell and the equivalent circuit model, as shown in Fig. 2 [24]. CNLS attempts to minimize the error between the measured impedance data and the calculated impedance data with a set of model parameters through iterative calculation to generate the best fitted parameter values. The complex impedance of the equivalent circuit model of the fuel cell in Fig. 2 at a certain frequency can be written as

$$Z(\omega) = f(\omega\ ;\theta_i);\quad \theta_i = R_{membrance},\ R_{cathode},\ C_{cathode}\,, \tag{10}$$

where $R_{membrane}$, $R_{cathode}$, and $C_{cathode}$ are the parameters of the equivalent circuit model for the fuel cell to be estimated by minimizing function Φ.

$$\Phi = \sum_{i=1}^{n}\left[\mathrm{Re}(y_i - Z_i)^2 + \mathrm{Im}(y_i - Z_i)^2\right] \tag{11}$$

The Taylor series method can be employed to calculate the value of impedance based on its previous value and the variation in the approximated parameters to implement the iteration calculation for the fitting algorithm. If the approximated parameters exhibit variation, Δ, the successive value of impedance can be obtained by using Taylor series expansion as

$$Z(\omega)_{j+1} = Z(\omega)_j + \frac{\partial Z(\omega)_j}{\partial\theta_i}\Delta\theta_i,\quad i = 1,2,3\,. \tag{12}$$

The values for $\Delta R_{membrane}$, $\Delta R_{cathode}$, and $\Delta C_{cathode}$, are then calculated with

$$\Delta\theta = A^{-1}.G\,, \tag{13}$$

where

$$A = \left[(Z_R)^T.Z_R + (Z_I)^T.Z_I\right],\ G = \left[(Z_R)^T.\Delta y_R + (Z_I)^T.\Delta y_I\right] \tag{14}$$

$$[Z_R]_{ij} = \mathrm{Re}\left(\frac{\partial Z_i}{\partial\theta_i}\right);\ [Z_I]_{ij} = \mathrm{Im}\left(\frac{\partial Z_i}{\partial\theta_i}\right);\ [\Delta y_R]_j = \mathrm{Re}(Y_i - Z_i);\ [\Delta y_I]_j = \mathrm{Im}(Y_i - Z_i)$$

This process can be performed by using an iterative method implemented in the DSP. In the first iteration loop, the value of Φ is calculated with the arbitrary initial value of the parameters. The variations in the parameters are calculated, and $R_{membrane}$, $R_{cathode}$, and $C_{cathode}$ are updated for the subsequent iteration. The calculation is repeated until the value of Φ converges to a certain limit, that is, 10^{-6} in this study [25], to obtain the best fitted value for the fuel cell model parameters.

3) Design of the Controller of the Proposed Converter for EIS Operation: In the EIS operation of the proposed system, main boost converter is utilized to generate current perturbation from the fuel cell for the impedance measurements. The bidirectional converter is utilized to regulate the output voltage of the system. The bidirectional converter with a battery is employed in the system to compensate for the power difference between the fuel cell output and the load occurring during the EIS operation by charging or discharging the battery. Therefore, the input and output of the power conditioning system can be completely decoupled in the proposed system, and the EIS operation can be performed regardless of the load variation.

The small-signal modeling technique is applied to obtain the transfer function of the converters [26]. In the modeling, a

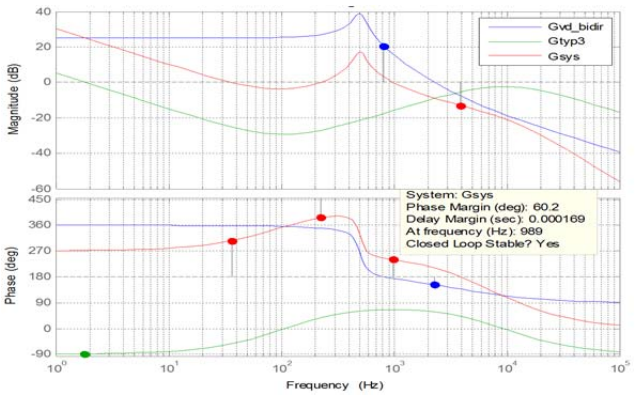

(a)

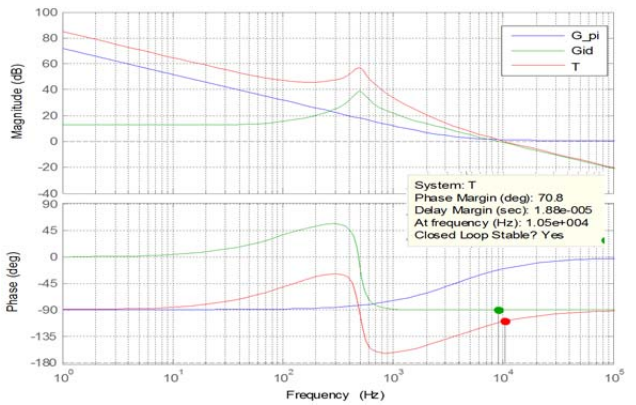

(b)

Fig. 3. Design of the controllers for each converter in the proposed system for EIS operation. (a) Bidirectional converter. (b) Boost converter.

voltage source in series with a resistor is used for the fuel cell model, and an R-C circuit is used for the battery model. The control to the fuel cell current (G_{id_boost}) transfer functions of the boost converter and the control to the output voltage (G_{vd_bidir}) transfer function of the bidirectional converter can be obtained as

$$G_{id\_boost}(s) = \frac{sV_oCR + (1-D)I_LR + V_o}{s^2LRC + s(L + CR_{fc}R) + R(1-D)^2 + R_{fc}}, \quad (15)$$

$$G_{vd\_bidir}(s) = \frac{-sI_{L2}L_2 + (1-D)V_o + R_{fc}I_{L2}}{s^2L_2RC + s(L_2 + CR_{fc}R) + R(1-D)^2 + R_{fc}}. \quad (16)$$

Considering that the control to the output voltage transfer function G_{vd_bidir} of the bidirectional converter operating in boost mode includes a right half-plane zero (RHPZ), the crossover frequency of the voltage loop that is less than one-third of the RHPZ frequency should be selected [27]. In this case, the RHPZ frequency of G_{vd_bidir} is 4.11 kHz; therefore, the crossover frequency is selected as 1.0 kHz. A type 3 compensator is used for voltage control in consideration of the requirement for phase boost.

In the design of the current controller of the boost converter for the fuel cell, selection of crossover frequency is important because the perturbation should not be distorted to obtain accurate impedance measurements. Given that the impedance measurements need to be performed from 0.1 Hz to 1 kHz to obtain a useful impedance spectrum, the bandwidth of the closed-loop system should be 10 times higher than the highest frequency of measurements to avoid distortion [28]. Thus, the bandwidth of the current loop is selected as 10.0 kHz in this case. The transfer function for each converter is obtained with the following parameters: nominal output voltage of the fuel cell, V_{fc} = 7.8 V; Li-ion battery voltage, V_b = 3.7 V; duty, D = 0.33; inductor for the boost converter, L_1 = 220.0 μH; inductor for the bidirectional converter, L_2 = 170.0 μH; output capacitor of the boost converter, C_{out} = 220.0 μF; equivalent capacitance of the battery, C_b = 40000.0 F; and equivalent series resistance of the battery, R_b = 30.0 mΩ.

Finally, a type 3 controller for the voltage control loop (G_{typ3_v}) and a proportional–integral (PI) controller for the current control loop (G_{pi_c}) are designed for the proposed converter as follows:

$$G_{typ3\_v}(s) = \frac{8.32\times10^{-7}s^2 + 0.0183s + 1}{2.45\times10^{-11}s^3 + 1.79s^2 + 0.032s}, \quad (17)$$

$$G_{pi\_c}(s) = \frac{1.037s + 2.37\times10^4}{s}. \quad (18)$$

Fig. 3 shows the bode plots of the open-loop transfer function, compensator, and closed-loop transfer function of the bidirectional converter (a) and boost converter (b). The closed loops are stable at the selected crossover frequency, with a sufficient phase margin.

IV. Design of the Controller of the Proposed Converter for the Load-Leveling Function for the Fuel Cell under Overload Condition

The fuel cell alone cannot provide robust source characteristics required for following the load instantaneously at significant load steps. This condition worsens when the fuel cell is associated with a fuel reformer to provide flexibility in the selection of the fuel because of its sluggish response characteristics [1]. Moreover, when the fuel cell is utilized to implement the power system, it is sized only to handle normal load to optimize the overall cost of the power system. Thus, when overload is applied to the fuel cell, it cannot be handled properly without the aid of an auxiliary energy storage device. Providing the load-leveling function by using auxiliary energy storage devices, such as batteries, is essential to make the power system associated with the fuel cell reliable. In the proposed system, a bidirectional converter associated with a Li-ion battery is adopted for the EIS operation and can be used to implement the load-leveling function by changing its control scheme in the normal mode operation as well.

When the fuel cell generates sufficient power to supply the load, the bidirectional converter is deactivated. Only the boost converter is activated to supply fuel cell power to the load through voltage control. When the overload condition occurs, the bidirectional converter is activated to supply power from

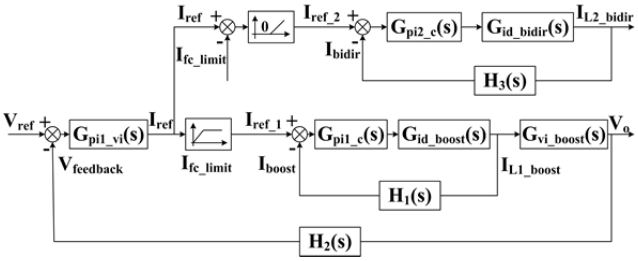

Fig. 4. Control scheme of the proposed converter for the load-leveling operation.

the battery together with the fuel cell. In this case, fuel cell power is limited to its rated power, and excess load power is supplemented by the auxiliary battery through the current control of the bidirectional converter. A control block diagram of the system in normal operation to achieve the load-leveling function is illustrated in Fig. 4.

In normal mode operation, the output voltage is regulated by a dual-loop controller to control both the inductor current and the capacitor voltage of the boost converter [29]. Thus, the control-to-inductor current transfer function (G_{id_boost}) and the control-to-output voltage transfer function (G_{vi_boost}) are derived through small-signal modeling in Equs. (19) and (20), respectively. Owing to the inherent characteristics of the dual-loop controller, the current-limiting function is easy to implement, which is required for the load-leveling function and to prevent the fuel cell from overloading. When implementing the load-leveling function, deriving the control-to-output current transfer function (G_{id_bidir}) for the bidirectional converter is also required. Accordingly, the function is derived by using the small-signal technique, as shown in Equ. (21).

$$G_{id\_boost}(s)=\frac{sV_oCR+(1-D)I_{L1}R+V_o}{s^2L_1RC+s(L_1+CR_{fc}R)+R(1-D)^2+R_{fc}} \quad (19)$$

$$G_{vi\_boost}(s)=-\frac{sRL_1I_{L1}+I_{L1}RR_{fc}-(1-D)RV_o}{sRCV_o+V_o+(1-D)RI_{L1}} \quad (20)$$

$$G_{id\_bidir}=\frac{V_{bat}\times\left[C_{out}C_bR_bs^2+\left(C_b+C_{out}\right)s\right]}{s^3L_2R_bC_bC_{out}+s^2L_2\left(C_b+C_{out}\right)++sR_bC_b+1} \quad (21)$$

In the design of the dual-loop controller, the bandwidth of the voltage loop (outer loop) must be lower than that of the current loop (inner loop) to ensure the dynamics of the control system [30]. In this case, the bandwidths of the outer and inner loops are set to 200Hz and 10 kHz, respectively.

Two PI controllers are utilized for voltage and current control as follows:

$$G_{pi1\_vi}(s)=\frac{0.2s+1431}{s}, \quad (22)$$

$$G_{pi1\_c}(s)=\frac{1.037s+2.37\times10^4}{s}. \quad (23)$$

Figs. 5(a) and 5(b) show the Bode plots for the inner and outer control loops of the dual-loop controller for the boost converter in normal mode operation.

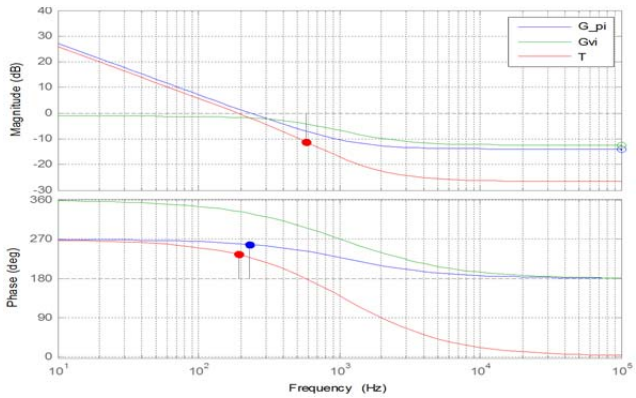

(a)

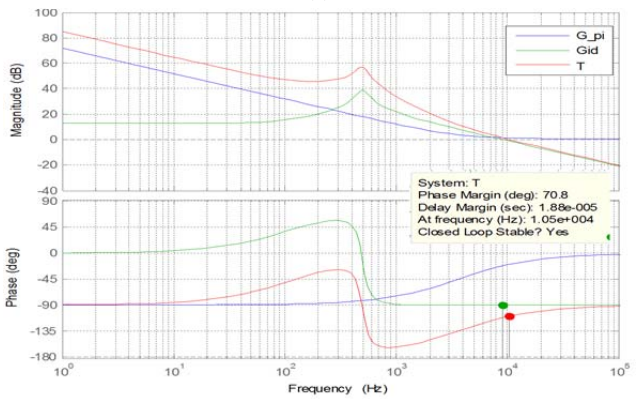

(b)

Fig. 5. Design of the dual-loop controller for the boost converter in normal mode operation. (a) Inner control loop. (b) Outer control loop.

A PI controller is also utilized to control the output current of the bidirectional converter for the load-leveling function. In this case, the bandwidth of the closed current loop is 3.0 kHz, and the transfer function of the PI controller is expressed as

$$G_{pi2\_c}(s)=\frac{0.2972s+2039}{s}. \quad (24)$$

V. Experimental Results of the Proposed Power Conditioning System for Fuel Cells

Fig. 6 shows the experimental setup for testing the functionality of the proposed system with a PEM fuel cell stack. The PEM fuel cell stack is built by CNL Energy, Seoul, Korea. The stack has 10 cells, and the membrane electrode assembly specifications are as follows: the membrane size is 5 × 5 cm^2, the membrane type is Nafion 212, and Pt catalysts for both anode and cathode. The fuel cell stack has a serpentine flow field configuration for both the anode and cathode, and its nominal electric output power is 110 W with water cooling. A 500 W PEM fuel cell-testing station manufactured by CNL Energy is used for a series of experiments, as shown in Fig. 6.

Fig. 7 shows the characteristic curve of the 110 W PEM fuel cell stack. As shown in the figure, the voltage of the fuel cell

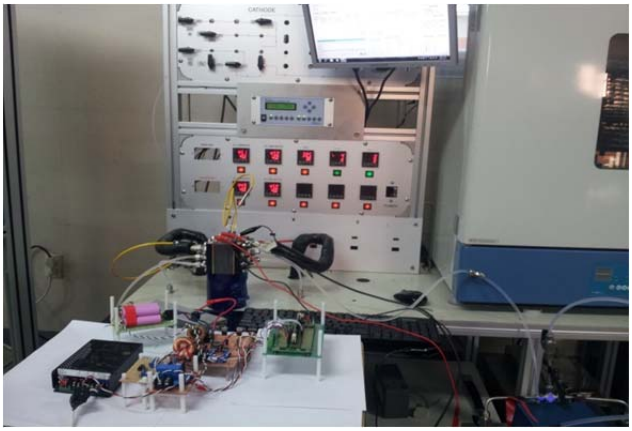

Fig. 6. Experimental setup for testing the functionality of the proposed system with a PEM fuel cell stack.

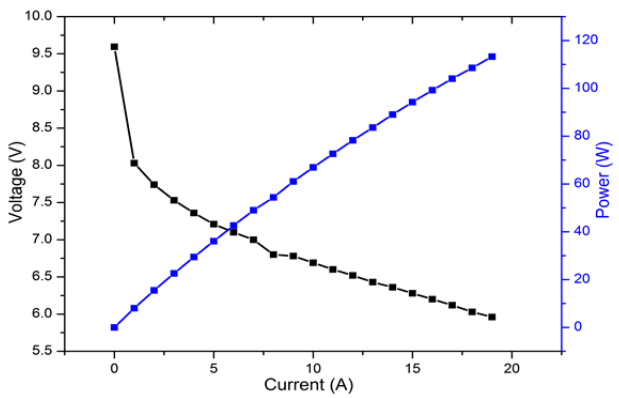

Fig. 7. Characteristic curve of the 110 W PEM fuel cell stack.

stack varies from 9.6 V to 5.96 V, and its maximum output current is 19 A at its rated output power.

Fig. 8 shows the performance of the proposed system during normal mode operation and EIS mode operation for the fuel cell stack. The load voltage is regulated at 12 V in both normal and EIS mode operations. In normal mode operation, the output voltage is controlled by the boost converter, and the bidirectional converter is deactivated, thereby resulting in zero output current from the five Samsung Li-ion 18650 cylindrical 3.7 V 2600 mAh (ICR18650-26F) batteries connected in parallel. The EIS operation is then performed to measure the AC impedance of the fuel cell stack at the operating point of 1.75 A. The amplitude of the perturbation current is 0.5 A in this case. When the EIS operation is initialized, frequency-swept current is generated by the current controller of the boost converter from the fuel cell stack for the impedance measurements; the bidirectional converter is utilized to regulate the output voltage. Given that the current perturbation is compensated for by charging/discharging the battery through the bidirectional converter, the output voltage can be regulated. No intervention exists between EIS operation and output voltage regulation. The operation of the proposed system is verified under varying conditions of the load. Considering that the load may vary during EIS operation for fuel cell diagnosis, the EIS operation has to be completely

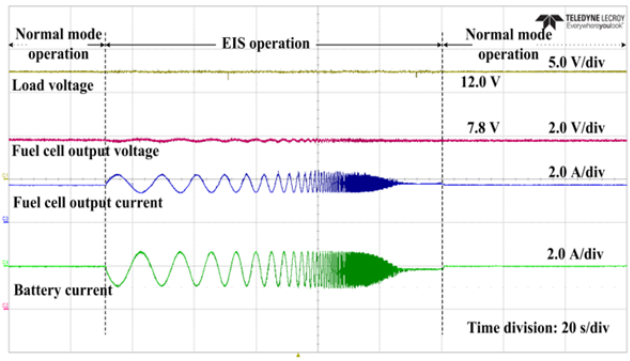

Fig. 8. Experimental waveforms of EIS operation under constant load condition.

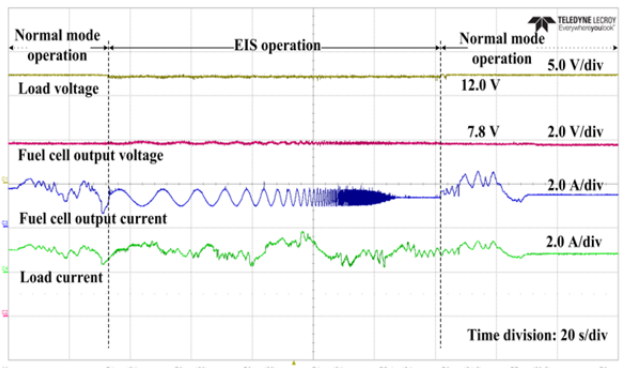

Fig. 9. Experimental waveforms of EIS operation under varying load condition.

decoupled from the load variation.

Varying load is applied to the system during EIS operation to verify the function. In this test, Kikusui PLZ1004W DC electronic load is used to vary the load. A randomly varying load scenario is also used for the test. Fig. 9 shows the operation of the proposed system under varying load conditions.

As shown in Fig. 9, the load voltage is regulated at 12 V precisely during EIS operation while the load is varying randomly. Fig. 9 also shows that under the varying load condition, the current perturbation applied to the fuel cell output has no interference from the load variation, thereby verifying the complete decoupling control of the proposed system.

Fig. 10 shows the Nyquist plots of the fuel cell measured at a certain operation point of 1.75 A. The accuracy of the measurement is verified by comparing the results obtained with the proposed system with those obtained with the WEIS500 workstation from WonATech, Seoul, Korea.

Fig. 10 clearly indicates that the two results are well-matched. The reduced chi-square value calculated with Equ. (25) is 0.96, which indicates a strong correlation between the two results.

$$\frac{\chi^2}{\nu} = \frac{\sum_{i=1}^{n}\left[\left(Z_{i\_m} - Z_{i\_weis}\right)/Z_{i\_m}\right]^2}{\nu\sigma^2}, \qquad (25)$$

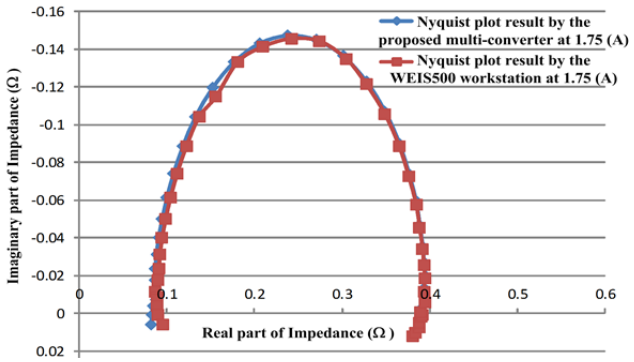

Fig. 10. Comparison of impedance spectra measured by the proposed system and WEIS500 workstation.

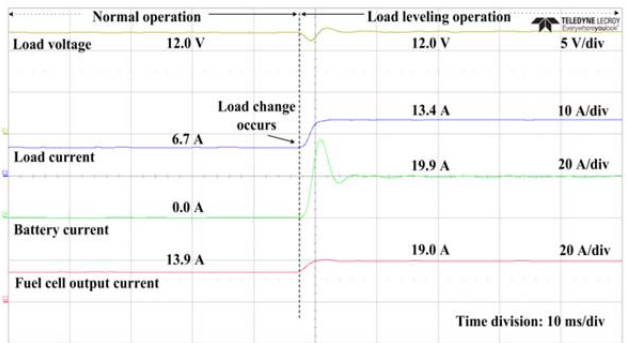

Fig. 11. Experimental result of the load-leveling function of the proposed system.

where

Z_{i_m}: impedance measured by the proposed converter,

Z_{i_weis}: impedance measured by the WEIS500 workstation,

σ^2: variance,

v: degree of freedom.

Fig. 11 shows the experimental results of the load-leveling function of the proposed system. When the load, which is larger than the rated power of the fuel cell stack (110 W in this case), is applied to the fuel cell stack, the load-leveling function is activated to avoid the overloading of the fuel cell stack by compensating for the excess power required by the load. In this experiment, the load-leveling operation is tested when the load is changed from 80 W to 160 W.

As shown in Fig. 11, when 80 W load is applied to the fuel cell stack, it can supply full power to the load, and the system operates in normal mode. No discharge current is provided by the auxiliary battery because the bidirectional converter is deactivated. However, when 160 W load (145% load) is applied, the fuel cell current is limited to 19 A by the current controller of the boost converter, and the battery is discharged to supply excess power to the load. Owing to the load-leveling function, the fuel cell stack can be protected from the overload, and the output voltage can be regulated at the desired value.

VI. Conclusion

A novel power conditioning system for fuel cell diagnosis and load leveling was developed. The impedance spectrum of the fuel cell stack was successfully measured by the proposed system even under the condition of varying load. The integrated load-leveling function protects the fuel cell stack from the overload, thereby improving the reliability of the fuel cell power system. The proposed system can be utilized to prognosticate the SOH of the fuel cell stack during operation, with no influence on the load.

References

[1] T. P. Kohler, D. Buecherl, and H. Herzog, "Investigation of control strategies for hybrid energy storage systems in hybrid electric vehicles," *Vehicle Power and Propulsion Conference*, pp.1687-1693, 2009.

[2] A. Khaligh and L. Zhihao, "Battery, ultracapacitor, fuel cell, and hybrid energy storage systems for electric, hybrid electric, fuel cell, and plug-in hybrid electric vehicles: State of the art," *IEEE Trans. Veh. Technol.*, Vol.59, No.6, pp. 2806-2814, Jul. 2010.

[3] R. O'Hayre, S.-W. Cha, W. Colella, and F. B. Prinz, *Fuel Cell Fundamentals*, 2nd ed., 2008.

[4] J. M. Miller, T. Bohn, T. J. Dougherty, and U. Deshpande, "Why hybridization of energy storage is essential for future hybrid, plug-in and battery electric vehicles," *Energy Conversion Congress and Exposition, 2009. ECCE 2009. IEEE* , pp. 2614-2620, 2009.

[5] D. S. Hyun, H. J. Hwang, D.-U. Kim, S. Hwang, Y.-H. Yun and B. S. Oh, "Development of an optimal charging algorithm of a Ni-MH battery for stationary fuel cell/battery hybrid system application," *International Journal of Hydrogen Energy*, Vol. 38, No. 21, pp. 9008-9015, Jul. 2013.

[6] C. Xie, J. M. Ogden, S. Quan, and Q. Chen, "Optimal power management for fuel cell–battery full hybrid powertrain on a test station," *Journal of Electrical Power & Energy Systems*, Vol. 53, pp. 307-320, Dec. 2013.

[7] J. Kim, I. Lee, Y. Tak, and B. H. Cho, "State-of-health diagnosis based on hamming neural network using output voltage pattern recognition for a PEM fuel cell," *International Journal of Hydrogen Energy*, Vol. 37, No. 5, pp. 4280-4289, Mar. 2012.

[8] T. Escobet, D. Feroldi, S. de Lira, V. Puig, J. Quevedo, J. Riera, and M. Serra, "Model-based fault diagnosis in PEM fuel cell systems," *Journal of Power Sources*, Vol. 192, No. 1, pp. 216-2231, Jul. 2009.

[9] Ju-hyung Lee, J.-H. Lee, W. Choi, K.-W. Park, H.-Y. Sun, and J.-H. Oh, "Development of a method to estimate the lifespan of proton exchange membrane fuel cell using electrochemical impedance spectroscopy," *Journal of Power Sources*, Vol. 195, No. 18, pp. 6001-6007, Sep. 2010.

[10] X. Yuan, J. C. Sun, M. Blanco, H. Wang, J. Zhang, and D. P. Wilkinson, "AC impedance diagnosis of a 500W PEM fuel cell stack: Part I: Stack impedance," *Journal of Power Sources*, Vol. 161, No. 2, pp. 920-928, Oct. 2006.

[11] X. Yuan, H. Wang, J. C. Sun, and J. Zhang, "AC impedance technique in PEM fuel cell diagnosis—A review," *International Journal of Hydrogen Energy*, Vol. 32, No. 17, pp. 4365-4380, Dec. 2007.

[12] M. Ciureanu, and R. Roberge, "Electrochemical impedance study of PEM fuel cells. experimental diagnostics and modeling of air cathodes," *The Journal of Physical Chemistry B*, Vol. 105, No. 17, pp. 3531-3539, Apr. 2001.

[13] S. M. R. Niya and M. Hoorfar, "Study of proton exchange membrane fuel cells using electrochemical impedance spectroscopy technique – A review," *Journal of Power Sources*, Vol. 240, pp. 281-293, Oct. 2013.
[14] J. J. Cooley, P. Lindahl, C. L. Zimmerman, M. Cornachione, G. Jordan, S. R. Shaw, and S. B. Leeb, "Multiconverter system design for fuel cell buffering and diagnostics under UAV load profiles," *IEEE Trans. Power Electron.*, Vol. 29, No. 6, pp. 3232-3244, Jun. 2014.
[15] J.-H. Kim, M.-H. Jang, J.-S. Choe, D.-Y. Kim, Y.-S. Tak, and B.-H. Cho, "An experimental analysis of the ripple current applied variable frequency characteristic in a polymer electrolyte membrane fuel cell," *Journal of Power Electronics*, Vol. 11, No. 1, pp. 82-89, Jan. 2011.
[16] M. Becherif, D. Hissel, S. Gaagat, and M. Wack, "Electrical equivalent model of a proton exchange membrane fuel cell with experimental validation," *Renewable Energy*, Vol. 36, No. 10, pp. 2582-2588, Oct. 2011.
[17] W. Choi, J. W. Howze, and P. Enjeti, "Development of an equivalent circuit model of a fuel cell to evaluate the effects of inverter ripple current," *Journal of Power Sources*, Vol. 158, No. 2, pp. 1324-1332, Aug. 2006.
[18] X. Changjun and Q. shuhai, "Drawing impedance spectroscopy for Fuel Cell by EIS," *Procedia Environmental Sciences*, pp. 589-596, 2011.
[19] M. Pérez-Page and V. Pérez-Herranz, "Study of the electrochemical behaviour of a 300 W PEM fuel cell stack by Electrochemical Impedance Spectroscopy," *International Journal of Hydrogen Energy*, Vol. 39, No. 8, pp. 4009-4015, 2014.
[20] S. Zhang, X. Yuan, H. Wang, W. Mérida, H. Zhu, J. Shen, S. Wu, and J. Zhang, "A review of accelerated stress tests of MEA durability in PEM fuel cells," *International Journal of Hydrogen Energy*, Vol. 34, No. 1, pp. 388-404, Jan. 2009.
[21] S. Ye, M. Hall, H. Cao, and P. He, "Degradation resistant cathodes in polymer electrolyte membrane fuel cells," *ECS Trans.*, Vol. 3, No. 1, pp. 657-666, 2006.
[22] W. Choi and J. Lee, "Development of the low-cost impedance spectroscopy system for modeling the electrochemical power sources," *7th International Conference on Power Electronics ICPE '07.*, pp. 113-118, 2007.
[23] J. Masciotti, J. Lasker, and A. Hielscher, "Digital lock-in detection for discriminating multiple modulation frequencies with high accuracy and computational efficiency," *IEEE Trans. Instrum. Meas.*, Vol. 57, No. 1, pp. 182-189, Jan. 2008.
[24] B. A. Boukamp, "A nonlinear least squares fit procedure for analysis of immittance data of electrochemical systems," *Solid State Ionics*, Vol. 20, No. 1, pp. 31-44, 1986.
[25] S. P. Manoharan, S. Bzrlasekaran, C. V. Sur, and Y. Yana, "Computer program for nonlinear least square analysis of impedance and admittance data," *Bulletin of Electrochemistry*, Vol. 2, No. 5, pp. 509-513, 1986.
[26] R. W. Erickson, and D. Maksimovic, *Fundamental of Power Electronics*, 2nd ed., Kluwer Academic, 2001.
[27] N. V. Sang and W. Choi, "A non-isolated boost charger for the Li-Ion battery suitable for fuel cell powered laptop computer," *7th International Power Electronics and Motion Control Conference (IPEMC)*, Vol. 2, pp. 946-951, 2012.
[28] T.-T. Nguyen, V.-L. Tran, and W. Choi, "Development of the intelligent charger with battery state-of-health estimation using online impedance spectroscopy," in *IEEE 23rd International Symposium on Industrial Electronics (ISIE)*, pp. 454-458, 2014.
[29] W.-Y. Choi, M.-K. Yang, and Y. Suh, "High-efficiency supercapacitor charger using an improved two-switch forward converter," *Journal of Power Electronics*, Vol. 14, No.1, pp. 1-10. Jan. 2014.
[30] O. Hegazy, J. V. Mierlo, and Philippe Lataire, "Analysis, modeling, and implementation of a multidevice interleaved DC/DC converter for fuel cell hybrid electric vehicles," *IEEE Trans. Power Electron.*, Vol. 27, No. 11, pp. 4445-4458, Nov. 2012.

Thanh-Tuan Nguyen was born in Ninh Binh, Vietnam, in 1987. He received his B.S. and M.S. degrees in mechatronics and electrical engineering from Vietnam National University, Vietnam, and Soongsil University, Republic of Korea, in 2010 and 2014, respectively. His research interests include modeling and control of DC–DC converters for renewable energy sources, diagnosis of electrochemical energy sources using electrochemical impedance spectroscopy, hybrid energy storage systems, and electric/hybrid electric vehicles.

Van-Tuan Doan was born in Hai Phong, Vietnam, in 1985. He received his B.S. and M.S. degrees in electrical engineering from Vietnam Maritime University, Vietnam, in 2008 and 2012, respectively. He is currently pursuing his Ph.D. degree in electrical engineering at Soongsil University, Republic of Korea. His research interests are DC/DC converters, power factor regulator converters, inverters, and soft-switching techniques for pulse-width modulation converters.

Woojin Choi was born in Seoul, Republic of Korea, in 1967. He received his B.S. and M.S. degrees in electrical engineering from Soongsil University, Republic of Korea, in 1990 and 1995, respectively. He received his Ph.D. degree in electrical engineering from Texas A&M University, USA, in 2004. He worked with Daewoo Heavy Industries as a research engineer from 1995 to 1998. In 2005, he joined the School of Electrical Engineering, Soongsil University. His research interests include modeling and control of electrochemical energy sources (e.g., fuel cells, batteries, and supercapacitors), power-conditioning technologies in renewable energy systems, and DC–DC converters for fuel cells and hybrid electric vehicles.